International Journal of Biological Macromolecules 145 (2020) 311–324

Contents lists available at ScienceDirect

International Journal of Biological Macromolecules

journal homepage: http://www.elsevier.com/locate/ijbiomac

A novel bioassay for the monitoring of hydrogen peroxide in human plasma samples based on binding of horseradish peroxidase-conjugated prostate specific antigen to poly (toluidine blue) as imprinted polymer receptor

Sanam Sardaremelli [a], Habib Razmi [a,*], Mohamad Hasanzadeh [b,*], Nasrin Shadjou [c,*]

[a] Analytical Chemistry Research Lab, Faculty of Basic Sciences, Azarbaijan Shahid Madani University, Tabriz, Iran
[b] Pharmaceutical Analysis Research Center, Tabriz University of Medical Science, Tabriz, Iran
[c] Department of Nanotechnology, Faculty of Science, Urmia, Iran

ARTICLE INFO

Article history:
Received 29 November 2019
Received in revised form 19 December 2019
Accepted 21 December 2019
Available online 24 December 2019

Keywords:
Binding
Bioassay
Protein
Prostate-specific antigen
Bioreceptor
Bioactivity

ABSTRACT

A low cost, sensitive and selective electrochemical imprinted biosensor for horseradish peroxidase-conjugated prostate-specific antigen (PSA) was designed and prepared based on the combination of Toluidine blue (TB) and self-assembly surface molecular imprinting technique. Poly toluidine blue [P(TB)] provided high surface area for dense loading of HRP-PSA antibody on GCE surface. P(TB), as supporting material, could effectively enhance imprinting efficiency and the electrode conductivity and facilitate electron transfer. The imprinted biosensor was characterized through Field emission scanning electron microscopy (FE-SEM), Energy-dispersive X-ray spectroscopy (EDX) and electrochemical methods. The proposed biosensor indicates very highly electrocatalytical activity for the reduction of hydrogen peroxide (H_2O_2). Also, engineered biosensor was used for determination of H_2O_2 by different electrochemical techniques including differential pulse voltammetry, square wave voltammetry and chronoamperometry. Under the optimized conditions, the proposed bio-imprinted polymer exhibit excellent electrocatalytical activity toward the reduction of H_2O_2 with wide linear range of 0.001 to 40 mM and a low limit of quantification (LLOQ) of 1 μM.

1. Introduction

Molecular imprinting technology has applied as an efficient way in relation to analytical separations, drug delivery, enzyme-like catalysis and chemical sensors [1,2]. In recent years, there are more attention for construction of the imprinting of complex bio macromolecules, in particular, proteins [3–13] because of their potential application in determination and electroactivity. Molecular imprinting technology is an important implement to prepare predesigned materials capable of recognizing and quantitatively detecting particular target molecules [7,8]. The essential components for the preparation of molecular imprinting polymer (MIP) are functional monomer, cross-linker, initiator and template [14,15]. The formation of MIP is achieved through non-covalent interactions such as hydrogen bonding, ion pair interactions or covalent interaction between the print molecule and the functional monomers [16] which among interactions non-covalent approach has been extensively popular due to some advantages of easily conducted procedure through synthesize, removal of template and a greater variety of functionalities into MIP sites [17]. After formation imprinted polymer, the template molecules are elutioned from the matrix of polymer. So the recognition sites and imprinted cavities are proportional to size and conformation of template molecules [18]. The formation of conventional MIP has been extensively applied for low molecular weight (<1500 Da) [19]. Forming imprinting large molecular weight encounter with some challenging such as slow mass transfer of the template to cross linker because of increasing the density of cross linker agent. Therefore, it brings about some problems like weak and slow rebinding kinetics,

* Corresponding authors.
E-mail addresses: h.razmi@azaruniv.ac.ir (H. Razmi), hasanzadehm@tbzmed.ac.ir (M. Hasanzadeh), n.shadjou@urmia.ac.ir (N. Shadjou).

https://doi.org/10.1016/j.ijbiomac.2019.12.195
0141-8130/

difficulty in removing template, and loose conformation of imprinted polymer [20]. To overcome above-mentioned weakness, surface molecular imprinting is appropriate solutions [21,22]. The surface molecular imprinting technique can solve embedding defects which occur in traditional MIP [23]. The material with binding Sites placed at the surface solve diffusion problem, such as leading to fast mass transfer and binding kinetics [24] and some general limitations for construction of the antibody format, including their large size. So, it is more likely to alter conformational and structure in related to antibodies [25]. In this work a novel and low-cost bio-imprinted polymer of horseradish peroxidase-conjugated prostate-specific antigen HRP-PSA was constructed based on surface imprinted polymer and can be successfully evaluated toward Hydrogen peroxide reduction. HRP is an important heme-containing enzyme which contains heme-iron and a neutral porphyrin ring which are vital for the structural and functional of enzyme. The maximum function of HRP activity is observed through pH 6 to 8 [26]. Poly Toluidine blue o (PTBs) has been used as substrate to immobilization of HRP-PSA due to its high stability and the easily electropolymerization on electrode surface. In recent decades there are more attention for coating of different monomers by electropolymerization [27–29]. From this prospect, electropolymerization of monomer leads to three-dimensional distribution of monomers which contribute to control thickness and the density of monomer on the surface of electrode [30]. It is important to point out that TBO is member of the thiazine group and water soluble family with an amino functional groups attached to phenothiazine ring which makes it feasible for electrochemical polymerization [31,32]. The polymerization of TB is done by one-electron oxidation of NH_2 to form cation radical which in next step Radical polymerization can happen between carbon-nitrogen interaction to form PTBs on the surface of electrode as shown in Scheme 1 [33]. PTBs provide a thin polymer film with efficient surface coverage which is necessary for subsequent imprinting bio receptor on the surface of a substrate in order to fabricating efficient MIP [34].

Therefore, in this research a facile and economical approach for the preparation of HRP-PSA surface molecular imprinting electrochemical biosensor has been suggested by spontaneously assembled molecular imprinting at PTBs. A simple and low cost bio-imprinted polymer was fabricated based on the combination of electrochemical polymerization of Toluidine blue and self-immobilization of surface molecular imprinting horseradish peroxidase-conjugated prostate-specific antigen (PSA) onto the glassy carbon electrode (GCE). Poly toluidine blue (PTB) provided high surface area for dense loading of HRP-PSA antibody on GCE surface. Also, engineered biosensor were used for determination of H_2O_2 by different electrochemical techniques. Finally, bio-imprinted polymer was satisfactorily applied for determination of H_2O_2 in unprocessed human plasma samples.

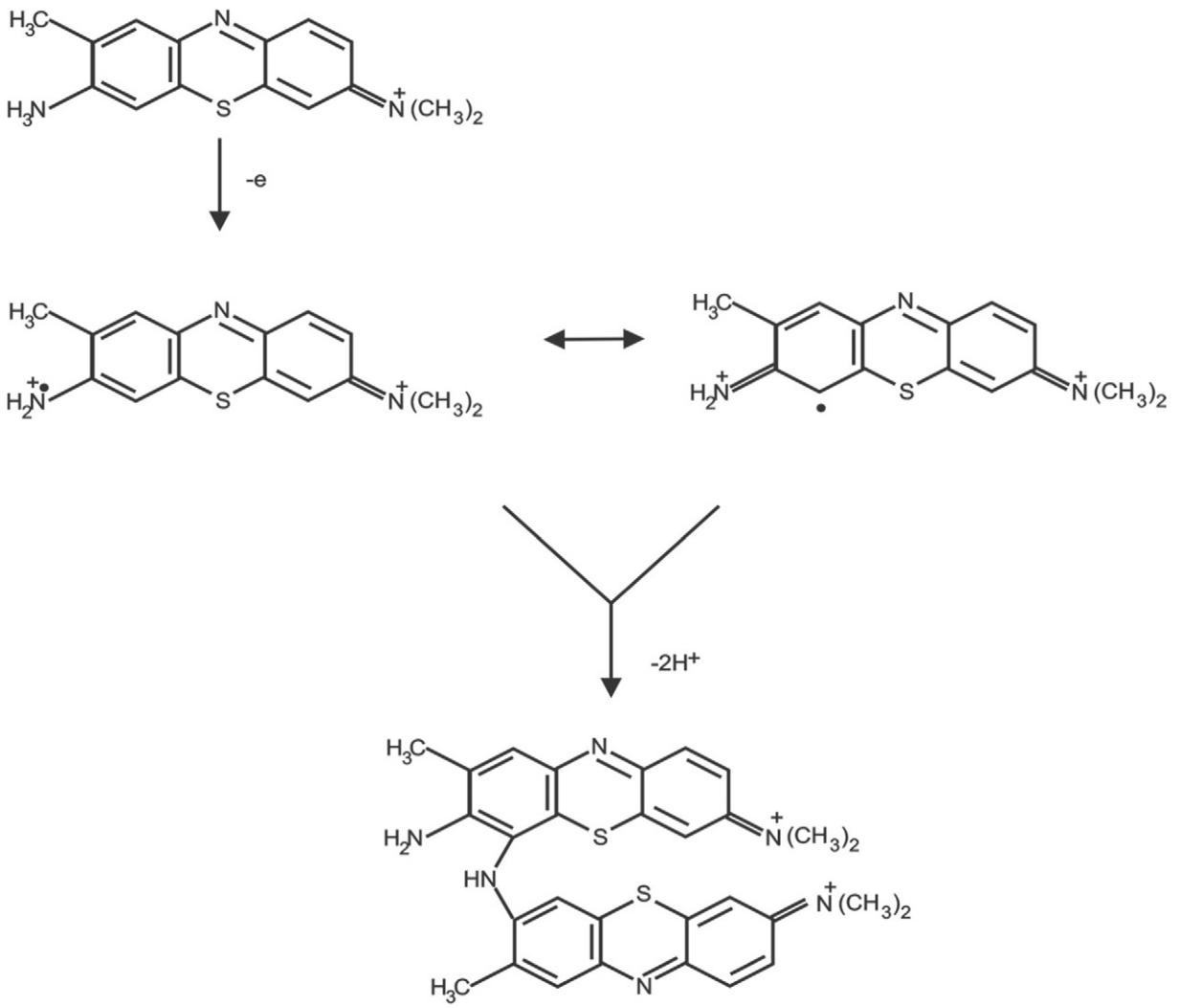

Scheme 1. Possible mechanism to electropolymerization of TBO.

2. Materials and methods

2.1. Chemical and reagents

Toluidine blue (C.I. 52040) was obtained from Merck Company. Hydrogen peroxide (30%) was purchased from Sigma-Aldrich Corporation. Potassium ferrocyanide $K_4Fe(CN)_6$, potassium ferricyanide $K_3Fe(CN)_6$, and KCl were purchased from Sigma-Aldrich (Ontario, Canada). HNO_3 and Hydrochloric acid (HCL) were purchased from Scharlau Chemie S.A. Phosphate buffer saline (PBS) solution (0.1 M) was prepared by Na_2HPO_4 (0.1 M) and NaH_2PO_4 (0.1 M) in deionized water. Human plasma samples were obtained from the Iranian Blood Transfusion Research Center (Tabriz, Iran). Horseradish peroxidase (HRP)-conjugated Prostate-specific antigen (PSA) antibody (anti-PSA) standard, standard buffer, and dilute solutions were obtained from CanAg Diagnostic AB Technology Co., (Gothenburg, Sweden). Human CA 15-3 ELISA kit (CanAg/CA15-3 EIA) including CA 15-3 antigen and Human Cancer Antigen CA125 ELISA Kit including CA 125 antigen were purchased from CanAg Diagnostic AB technology Co., (Gothenburg, Sweden).

2.2. Apparatus

Electrochemical measurements were runner with a computer-controlled electrochemical system comprising of AUTOLAB system with PGSTAT302N (Eco Chemie, Utrecht, The Netherlands) using NOVA 1.11 software. The conventional three-electrode electrochemical cell was used by glassy carbon electrode (GCE), Ag/AgCl and a platinum wire as the working, reference, and counter electrodes, respectively.

Electrochemical characterization of bio-imprinted polymer was carried out by CV technique using $Fe(CN)_6^{4-}/Fe(CN)_6^{3-}$ (1 mM) in the potential range from −1 to 1 V at a scan rate of 50 $mV \cdot s^{-1}$. In addition, evaluation and determination of H_2O_2 using bio-imprinted polymer has been investigated by DPV, SWV and chronoamperometry techniques in 0.1 M PBS solution (pH 7.4) containing different concentration of H_2O_2.

The surface morphology of the electrode surface was characterized by a high-resolution field emission scanning electron microscope (FE-SEM, Hitachi-SU8020, Czech) with an operating voltage of 3 kV. Chemical compositions of the electrode were analyzed by an energy dispersive spectroscopy (EDS) coupled with the FE-SEM equipment.

2.3. Electropolymerization of TB on the surface of GCE

The GCE was carefully polished with 0.3 and 0.05 μm of alumina aqueous slurry. Then, GCE was cleaned ultranistically in 1:1 nitric acid solution, alcohol and redistilled water, respectively. PTBs were formed during the electropolymerization of 0.5 mM TBs in PBS (pH = 7.4) using CV technique. The modification process was performed in the potential range of −0.5 to 0.15 V at sweep rate of 50 mV/s using 25 scan number. After polymerization of TBs on the surface of GCE, the obtained electrode rinsed with deionized water to remove unabsorbed TBs. Fig. 1 indicates CVs of GCE in the polymerization process. By stabilization potential among a region of −0.5 to 0.15 V a simple CVs corresponding to the cathodic reactions of TB with the formal potential of −0.24 V and anodic reaction of TBs with a potential −0.22 V are observed. The peak currents increase with successive scanning, indicating an increase in the quantity of electroactive species on the surface of GCE, and leading to form PTBs films formation.

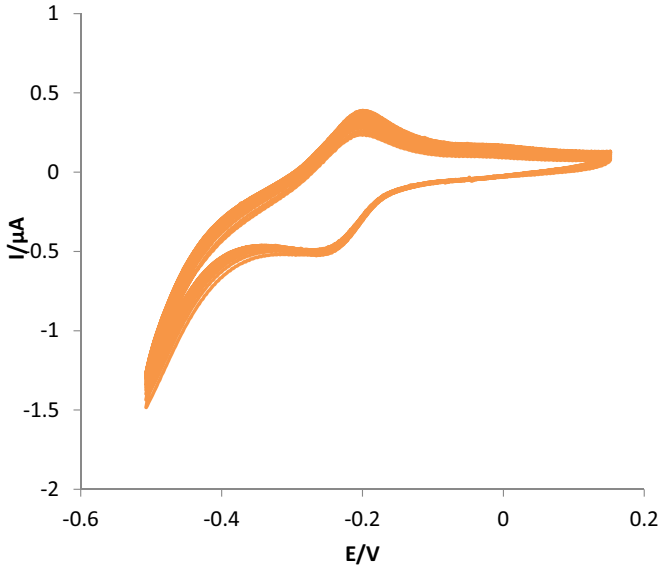

Fig. 1. CVs of GCE in the presence of 0.5 mM of TB in 0.1 M PBS (pH 7.4) at 50 mV/s^{-1}. Number of cycle = 25.

2.4. Fabrication of biosensors based on HRP(PSA)-PTBs imprinted polymer

The preparation procedure of bio-imprinted polymer is presented in Scheme 2. The obtained PTBOs/GCE was immersed in a PBS (pH = 6.5) containing 0.06 μg/ml of HRP-anti-PSA for 24 h in a refrigerator at 4 °C. HRP-PSA template molecules were easily immobilized on PTBs matrix by hydrogen bond interaction between the –COOH groups of the HRP molecules and the $–NH_2$ groups of the PTBs film. The removal of the molecular template were carried out in continuously stirred 1.0 M hydrochloric acid solution for 15 min.

3. Results and discussion

3.1. Morphology and elementary analysis of bio-imprinted sensors

FE-SEM was used to characterizing surface morphology of PTBs/GCE, HRP(PSA)/PTBs/GCE and MIP/PTBs/GCE. As shown in Fig. 2A, the polymerized TBO were stained with aligned chain (branch, dendrite) like on the surface of GCE which enable highly dense PTBs for subsequent imprinting of target molecule. The elements carbon, nitrogen, Phosphore and Sulphur with their corresponding weight percentages of 89.10, 9.66, 0.65 and 0.59 were obtained by the EDX spectrum. It can be apparently seen that the considerable weight percentages of carbon, nitrogen, phosphor and Sulphur were acquired from the formed PTBs on the surface of electrode.

Fig. 2B indicates the loading of the enzyme-conjugated antibody on the surface of PTBs/GCE, As it can be seen, the morphology of the electrode surface was changed, indicating a successful assemble of template on the surface of PTBs/GCE. According to EDS, the different percentages of carbon, nitrogen, oxygen and phosphore compare to matrix polymer have observed. EDS analysis confirmed FE-SEM results.

Fig. 2C shows that when the template HRP-PSA molecules were eliminated from the matrix of polymer, a uniform and films of PTBs with cavities are obvious on the surface of electrode which prove the successful formation of MIP/PTBs/GCE.

3.2. Electrochemical characterization

CVs measurement was conducted for the characterization of HRP (PSA)-imprinted biosensors. CVs scanning was performed in a 1.0 mM

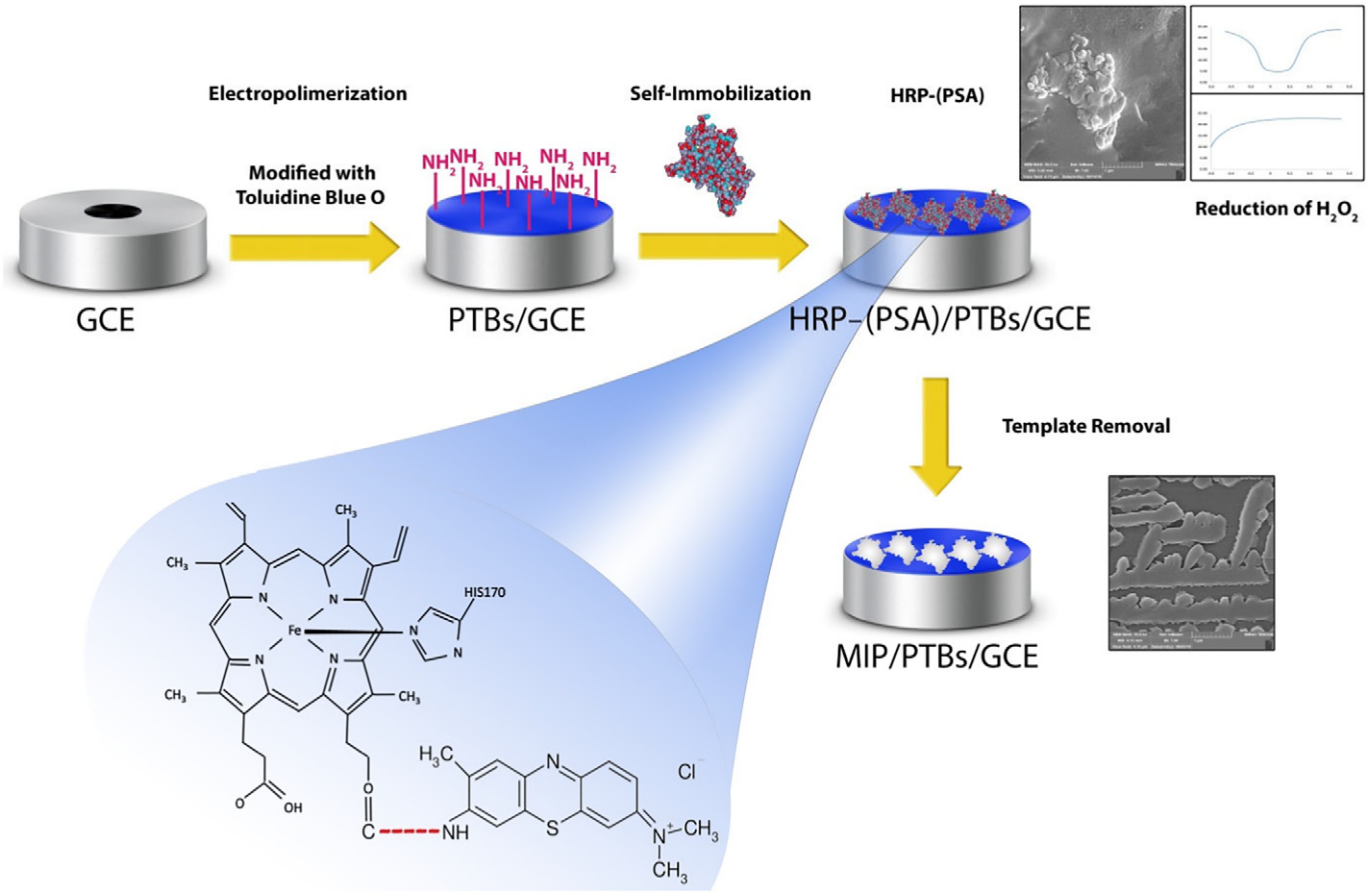

Scheme 2. The preparation procedure of HRP-(PSA) imprinted polymer based biosensor

of $K_3[Fe(CN)_6]/K_4[Fe(CN)_6]$ solution containing 0.1 M KCl as support electrolyte. Fig. 3 indicate a pair of well-defined redox peaks for bare GCE. When GCE was modified by PTBs, the peak current of PTBs/GCE increased obviously as seen in Table 1. The cathodic current increasing indicates that PTBs with excellent conductivity can accelerate electron shuttle of $Fe(CN)_6^{4-}/Fe(CN)_6^{3-}$ when HRP(PSA) template were assembled on stained PTBs/GCE through hydrogen bond interaction between the –COOH groups and the $-NH_2$ groups of the PTBs the response current of the obtained electrode dramatically decreased which presents the immobilization of HRP(PSA) antibody is carried up successfully and retracted electron transfer. When the template protein molecules were eliminated from the three-dimensional matrix, the particular cavity of HRP(PSA) molecules were re-constructed after elution. The peak currents of MIP/PTBs/GCE obviously decreased again compared to HRP(PSA)/PTBs/GCE electrode because the negatively charged of the obtained MIP polymer causes repulsive interaction with the supporting electrolyte (Fig. 4).

The elution of molecular template has been investigated in different times and obviously observed that after the 15 min the current peak has not changed so 15 min selected as optimum time for elimination of target.

3.3. Kinetic studying

Kinetic study evaluates various factor which effect the rate of reaction, reversibility and surface coverage [35]. In this regard, typical CVs of PTBs/GCE were recorded at different scan rate from 10 to 500 $mV \cdot s^{-1}$ in $Fe(CN)_6^{4-}/Fe(CN)_6^{3-}$ solutions. As can be seen in Fig. 5A the peak currents was increased with increasing of scan rate. The results implied that electrochemical kinetic for PTBs is involved in controlled process. For evaluation the efficient surface coverage of electrode, the special surface of GCE coated by PTBs should be studied. The surface coverage of modified electrode was calculated by studying the effect of sweep rates on the peak currents using Eq. (1) (Fig. 5E) [36–38]:

$$I_p = \left(F^2 n^2 / 4RT\right) \nu A \Gamma * \quad (1)$$

which n is equal of the number of electron transferred involved in reaction, F is Faraday constant, R is considered as ideal gas constant (8.3144 J/mol K) and T is considered as temperature (K).

Γ^* represent the surface coverage of the modified electrode (M/cm^2), ν being the potential sweep rate and A is the electrode surface area ($A = \pi r^2 = 0.0314\ cm^2$). The surface coverage of PTBs/GCE was obtained as $5.1 \times 10^{-9}\ cm^2 \cdot s^{-1}$ which provide an efficient surface for the immobilization of HRP(PSA) and formation of bio imprinted polymer. According to Fig. 5C it is concluded that the PTBs/GCE is in the irreversible reactions. Therefore, the electron transfer in the redox reaction of PTBs/GCE is irreversible. According to dependency of Neperian logarithm of peak current *versus* Neperian logarithm of sweep rate in Fig. 5D a slop approximate to 1 is considered as absorption and a gradient close to 0.5 is considered as the diffusion controlled by Fick's law. So mass transfer was controlled by diffusion [39,40].

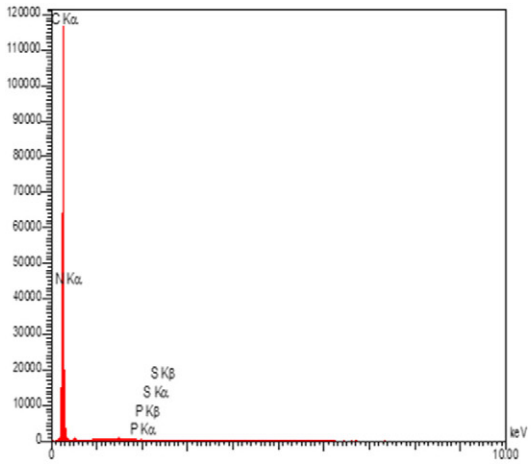

Elt	Int	W%	A%
C	6647.9	89.10	91.05
N	61.7	9.66	8.46
P	43.9	0.65	0.26
S	40.7	0.59	0.23

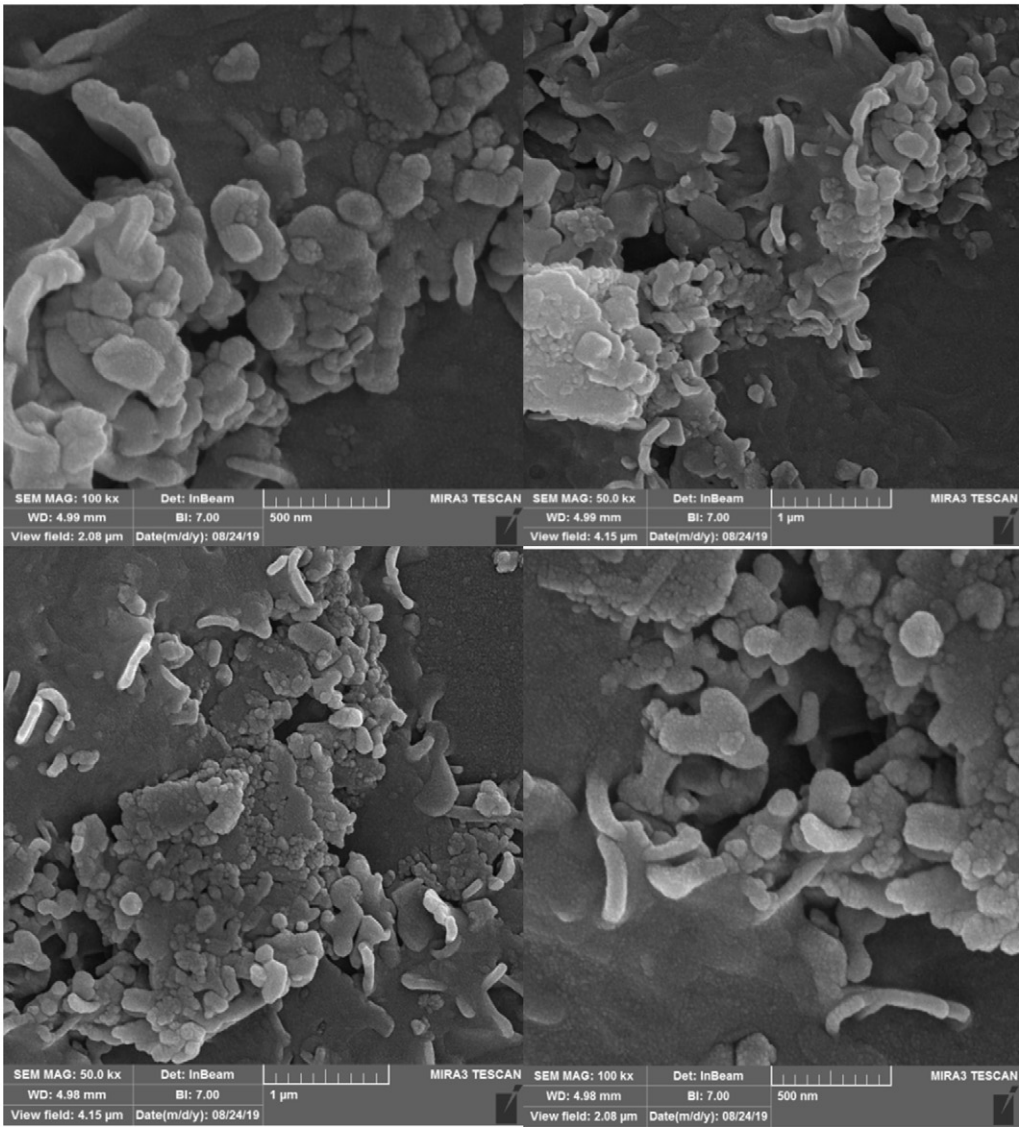

Fig. 2. A. FE-SEM images of PTBs/GCE at different magnifications along with EDX. B. FE-SEM images of HRP-(PSA)/PTBs/GCE at various magnifications along with EDX. C. FE-SEM images of MIP/PTBs/GCE at various magnifications along with EDX.

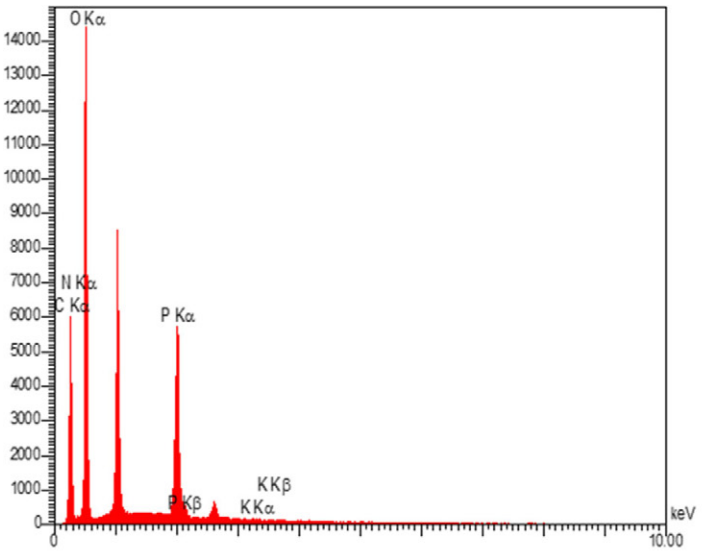

Elt	Int	W%	A%
C	501.9	26.5	34.3
N	27.3	1.93	2.18
O	1424.5	56.18	55.4
P	895.1	15.13	7.72
K	34.2	0.61	0.2

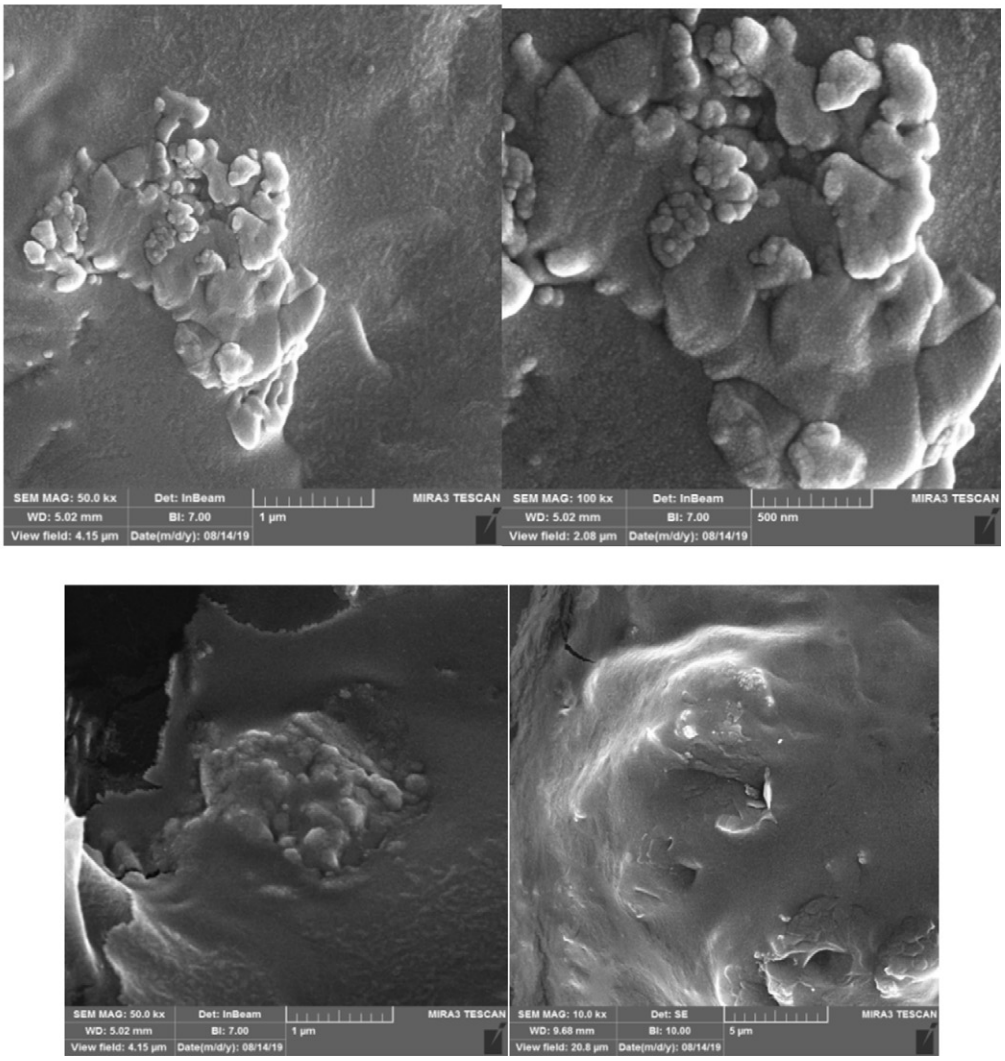

Fig. 2 (*continued*).

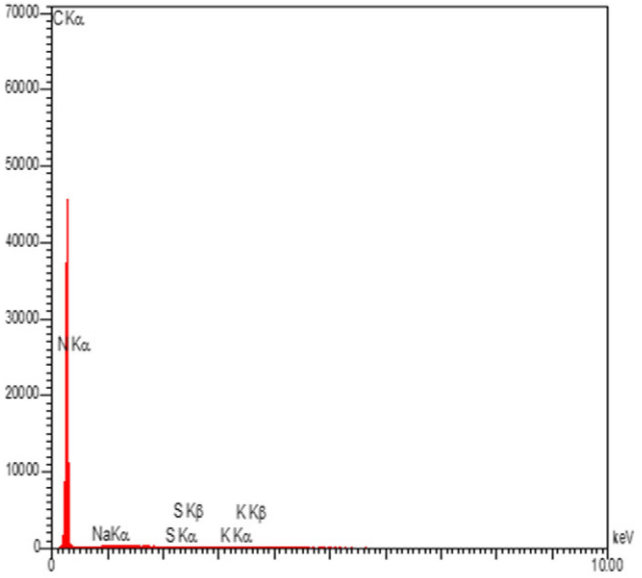

Elt	Int	W%	A%
C	6647.9	90.47	92.65
N	61.7	7.20	8.46
S	40.7	0.82	0.31

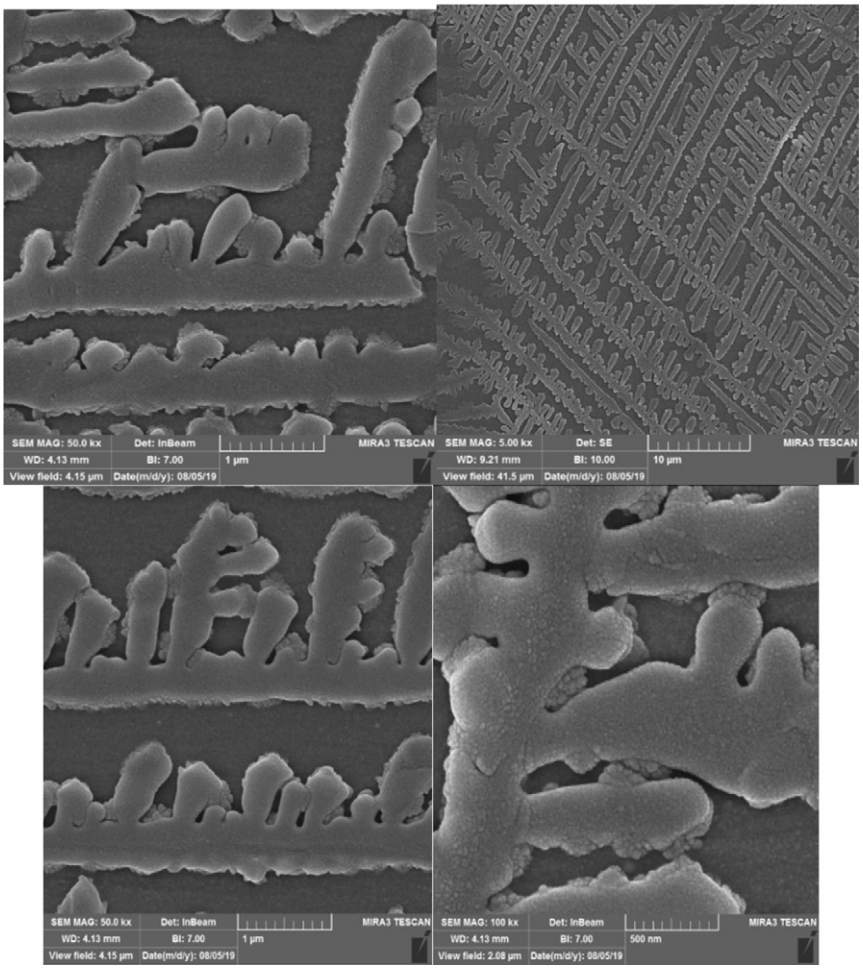

Fig. 2 (*continued*).

3.4. Electrocatalytical activity of the HRP(PSA) imprinted sensor

The electrocatalytical behavior of HRP(PSA) imprinted sensor toward hydrogen peroxide reduction was evaluated in PBS solution with different concentration of H_2O_2 by DPV, SWV and chronoamperometry techniques. The electrocatalytical activity of bio-imprinted sensor toward H_2O_2 reduction was also evaluated by CV (Fig. 6) to obtain the appropriate potentials for

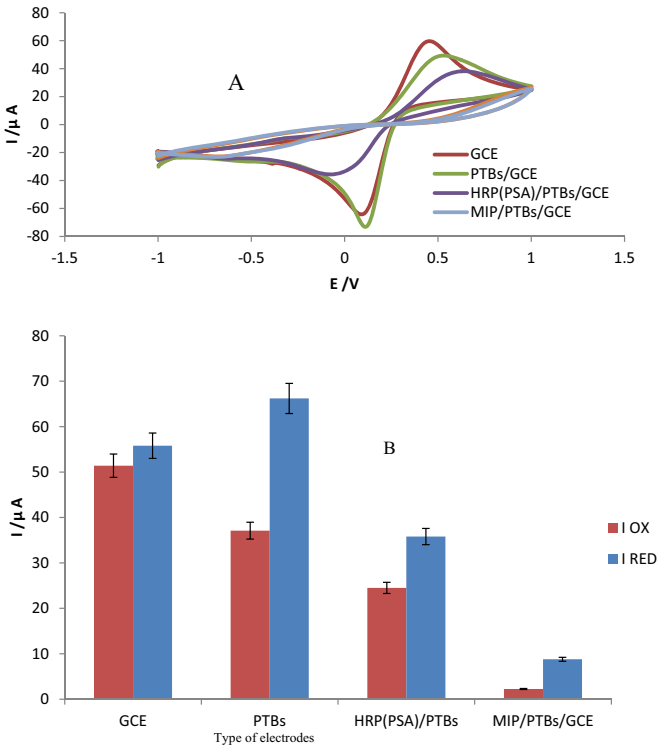

Fig. 3. A) CVs of GCE.PTBs/GCE, HRP(PSA)/PTBs/GCE, and MIP/PTBs/GCE in 1 mM $Fe(CN)_6^{4-}/Fe(CN)_6^{3-}$ containing 0.1 M KCl at a scan rate of 50 mV/s. B) Histogram of peak currents *versus* different type of electrodes.

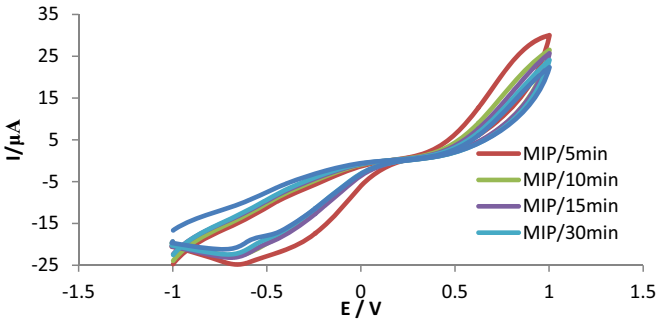

Fig. 4. CVs of MIPs based biosensor in different elution times (5, 10, 15, 30 and 45 min). Sweep rate was 50 mV/s.

chronoamperometry analysis which −0.80 V was selected as optimum potential to chronoamperometry studies. As shown in Fig. 7 reduction peak currents increased gradually with the successive increase of H_2O_2 concentration, which illustrated the bioelectrocatalytical activity of bio-imprinted polymer toward the reduction of H_2O_2. The current response was investigated from the concentration of H_2O_2 from 0.001 to 40 mM using DPV and SWV techniques. The linear range for H_2O_2 was obtained as 0.001 to 40 mM by DPV which regression equations are $-I(\mu A) = 0.0117C_{[H2O2](mM)} + 0.0136$. $R^2 = 0.9916$ and $-I(\mu A) = 0.8582C_{[H2O2](mM)} + 1.33$. $R^2 = 0.9952$ by SWV. In addition, the linear range obtained by chronoamperometry technique was 0.001 to 10 mM which regression equation was $-I(\mu A) = 0.2588C_{[H2O2](mM)} + 0.3619$, $R^2 = 0.9912$.

The current response could be attributed to reduction of heme-oxygen complex as oxidized form [41,42]. The lower limit of quantification (LLOQ) for determination of H_2O_2 using MIP based biosensor was obtained as 0.001 mM (Fig. 8).

3.5. Real sample analysis

The fabricated bio-MIP was also successfully used for measuring of H_2O_2 in human plasma by using DPV, chronoamperometry and SWV techniques (Fig. 9).

Table 1
Peak currents and potential of different steps of electrode preparation.

	E°_{OX}/V	E°_{RED}/V	I_{OX}/μA	I_{RED}/μA
GCE	0.4	0.1	51.4	−55.8
PTBs/GCE	0.5	0.11	37.1	−66.2
HRP(PSA)/PTBs/GCE	0.6	−0.04	24.5	−35.8
MIP/PTBs/GCE	0/84	−0.6	2.24	−8.79

To investigate of the practical application of bio-imprinted polymer, different concentrations of H_2O_2 were spiked into human plasma samples and determined by DPVs, SWVs and chronoamperometry techniques.

As shown in Fig. 10 engineered MIP-based biosensor has ability for determination of H_2O_2 in the concentration range of 0.005 to 25 mM and the calibration curve plotted to the linear regression equation is as follows:

$$-I(\mu A) = 2.8651C_{[H2O2](mM)} - 2.7747, R^2 = 0.8615 \text{ by SWV}$$

$$-I(\mu A) = 0.8699C_{[H2O2](mM)} + 0.5519, R^2 = 0.9206 \text{ by Chronoamperometry}$$

$$-I(\mu A) = 0.0323C_{[H2O2](mM)} - 0.0157, R^2 = 0.9083 \text{ by DPV}$$

The good LLOQ mainly depended on the good recognition capability of the imprinted sensor and the remarkable biocompatibility of P(TB). The LLOQ is lower than those of previously reported electrochemical method based on HRP/o-phenylenediamine/H_2O_2/graphite-epoxy composite, fluorometry based on microfluidic paper-based devices, chemiluminescence based on surface imprinting based on phenylboronic acid functionalized ionic liquid@magnetic graphene oxide and multichannel ink-jet ejection system, flow injection analysis and spectrophotometric methods based on *o*-phenylenediamine, and bromopyrogallol red.

It is important to point out that, forming imprinting large molecular weight encounter with some challenging such as slow mass transfer of the template to cross linker because of increasing the density of cross linker agent. Therefore, it brings about some problems like weak and slow rebinding kinetics, difficulty in removing template, and loose conformation of imprinted polymer [20]. To overcome above-mentioned weakness, surface molecular imprinting is appropriate solutions [21,22]. The surface molecular imprinting technique can solve embedding defects which occur in traditional MIP [23]. The material with binding Sites placed at the surface solve diffusion problem, such as leading to fast mass transfer and binding kinetics [24] and some general limitations for construction of the antibody format, including their large size. So, it is more likely to alter conformational and structure in related to antibodies [25]. In this work a novel and low-cost bio-imprinted polymer of horseradish peroxidase-conjugated prostate-specific antigen HRP-PSA was constructed based on surface imprinted polymer and can be successfully evaluated toward Hydrogen peroxide reduction. HRP is an important heme-containing enzyme which contain heme-iron and a neutral porphyrin ring which are vital for the structural and functional of enzyme. The maximum function of HRP activity is observed through pH 6 to 8 [26]. Poly Toluidine blue o (PTBs) has been used as substrate to immobilization of HRP-PSA due to its high stability and the easily electropolymerization on electrode surface. In

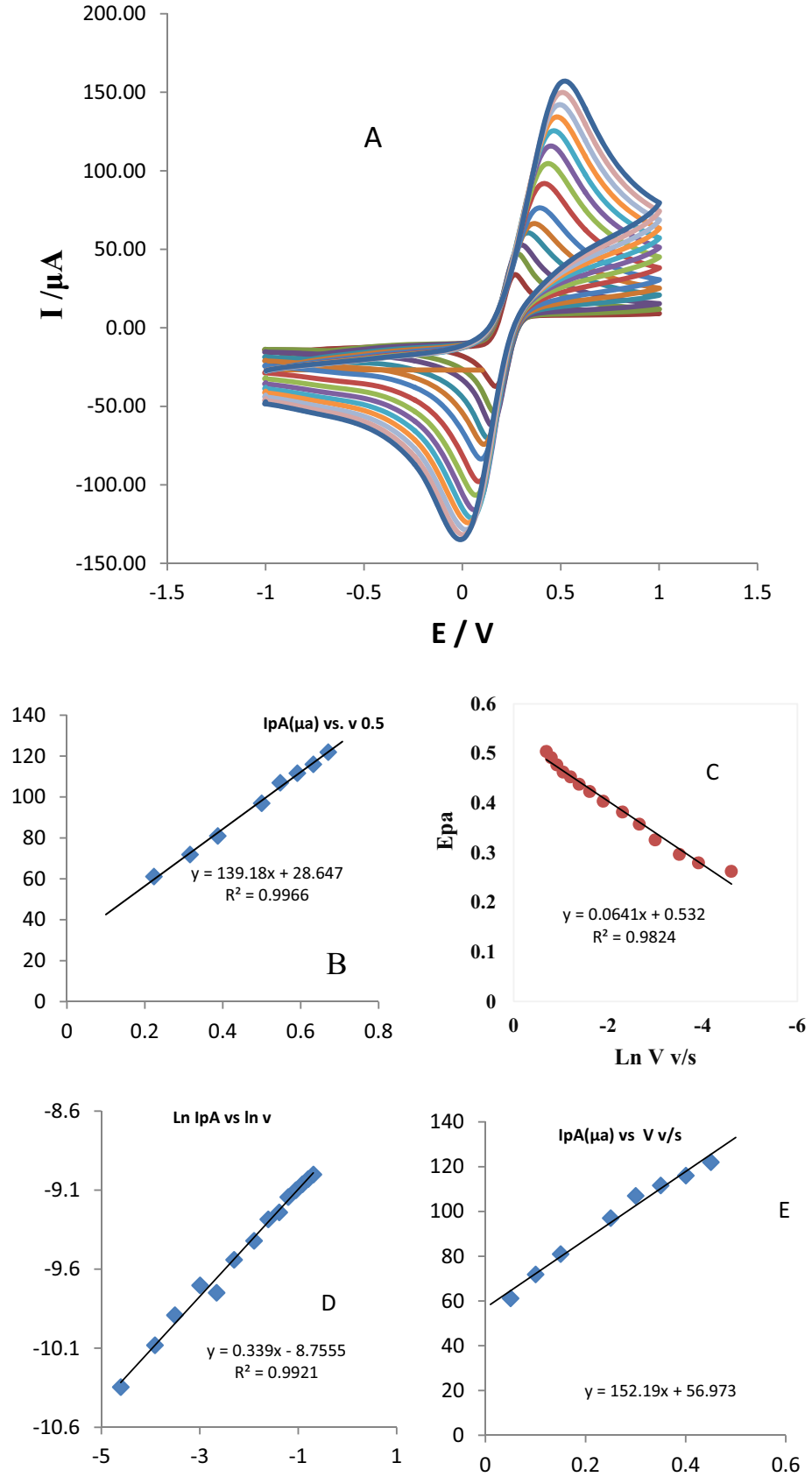

Fig. 5. A) CVs of PTBs/GCE in 1 mM of $Fe(CN)_6^{4-}/Fe(CN)_6^{3-}$ containing 0.1 M KCl. B) variation of peak currents *versus* square roots of scan rates. C) Dependency of peak potential *versus* Neperian logarithm of sweep rate. D) Variation of Lnlp *versus* Lnv. E) Dependency of peak currents *versus* sweep rates.

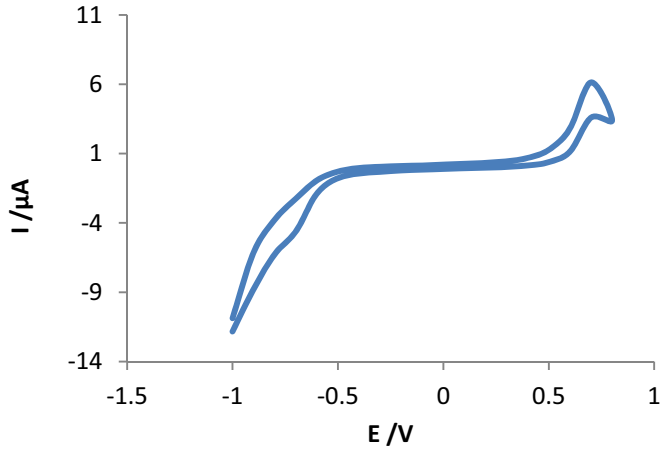

Fig. 6. CVs of HRP-PSA imprinted sensor in PBS solution (pH = 7.4) including of H_2O_2. Sweep rate is 50 mV/s.

recent decades there are more attention for coating of different monomers by electropolymerization [27–29]. From this prospect, electropolymerization of monomer leads to three-dimensional distribution of monomers which contribute to control thickness and the density of monomer on the surface of electrode [30]. It is important to point out that TBO is member of the thiazine group and water soluble family with an amino functional groups attached to phenothiazine ring which makes it feasible for electrochemical polymerization [31,32]. The polymerization of TB is done by one-electron oxidation of NH_2 to form cation radical which in next step Radical polymerization can happen between carbon-nitrogen interaction to form PTBs on the surface of electrode as shown in Scheme 1 [33]. PTBs provide a thin polymer film with efficient surface coverage which is necessary for subsequent imprinting bio receptor on the surface of a substrate in order to fabricating efficient MIP.

3.6. Evaluation of stability

The stability of PTBs film was investigated after 2, 10, 50, and 100 cycles in 1 mM of Fe $(CN)_6^{-3-/4-}$ as mediator solution. As seen in Fig. 11,

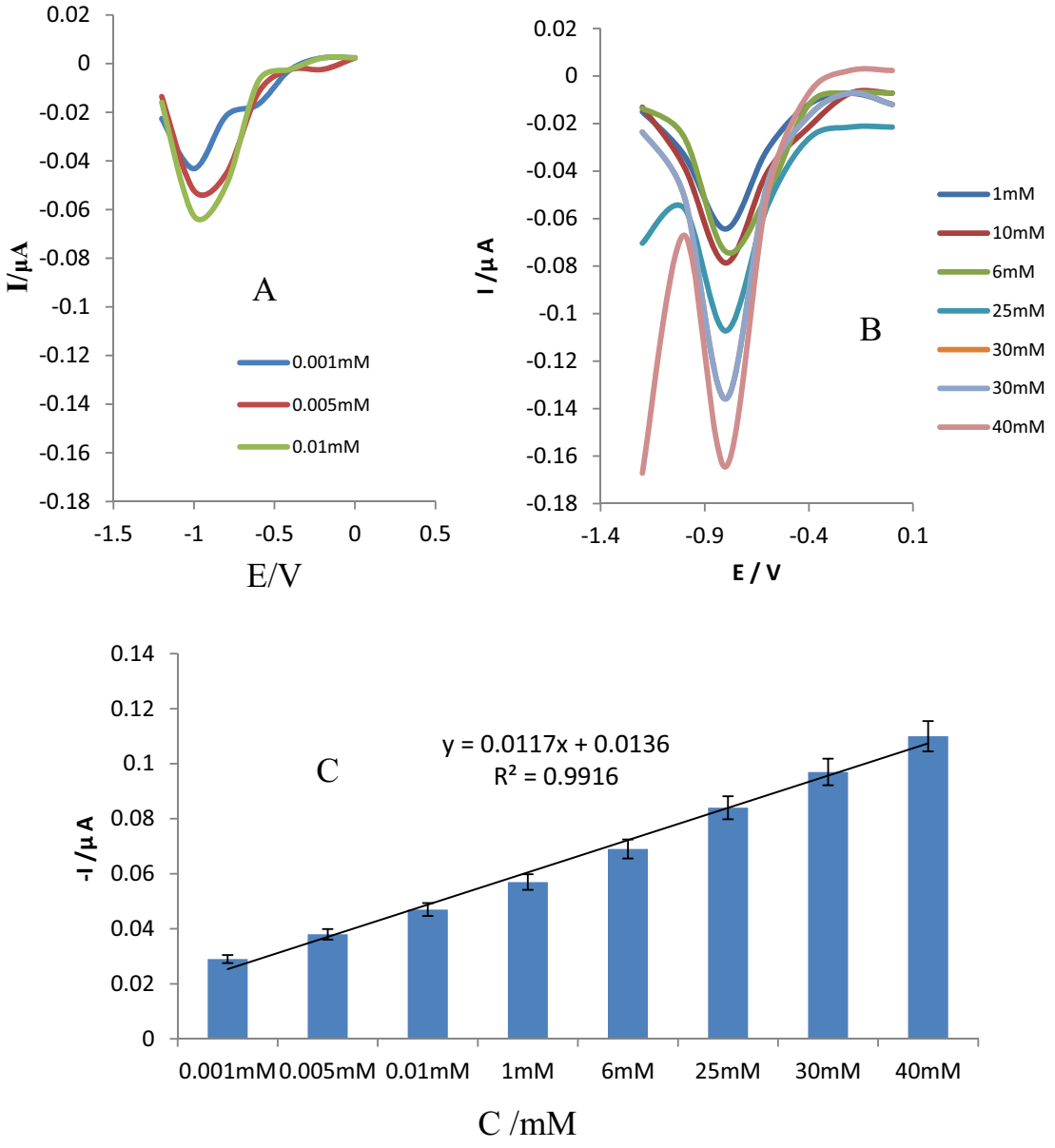

Fig. 7. A, B) DPVs responses HRP(PSA)/PTBs based biosensor toward reduction of H_2O_2 in different concentration from 0.001to 40 mM. C) Calibration curve.

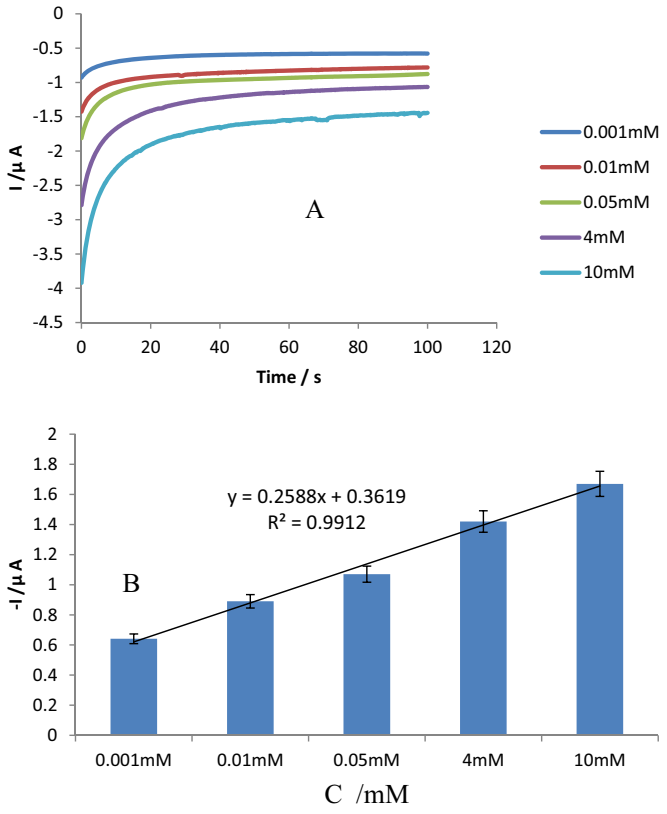

Fig. 8. A) Chronoamperometry response of the HRP(PSA)/PTB s based biosensor in different concentration of H_2O_2 from 0.001to 10 mM. B) Calibration curve.

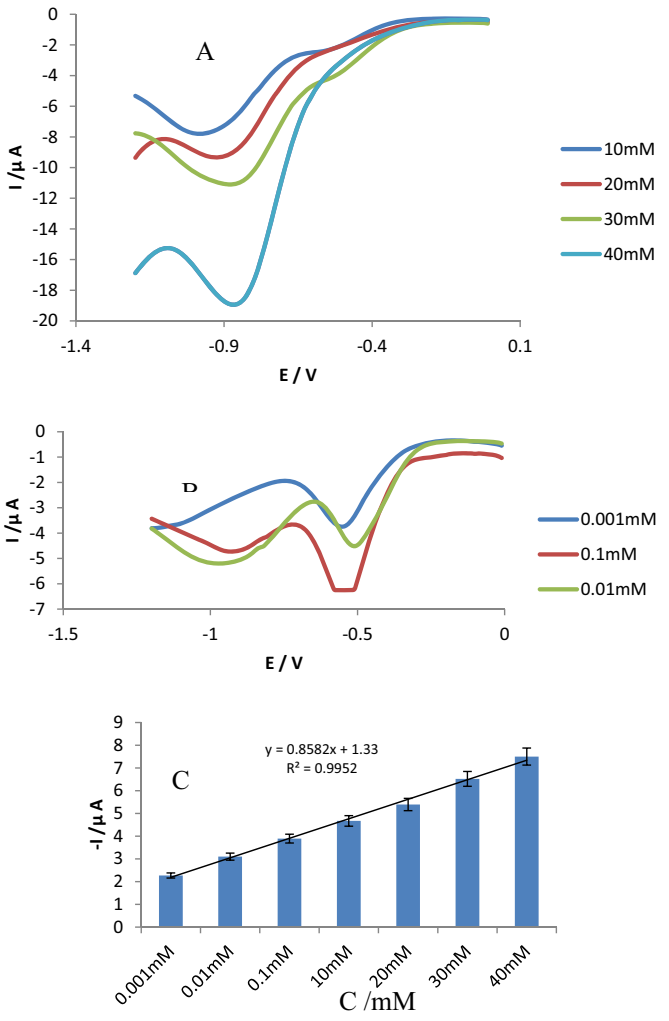

Fig. 9. (A, B) SWVs response of HRP(PSA)/PTBs-based biosensor in different concentration of H_2O_2. C) Calibration curve.

good cycle stability was obtained after 10 cycles which shows excellent function of PTBs after 10 cycles. However, there was little change in the oxidation and reduction potentials of the obtained polymer, after 50 cycles. It is found that redox peak currents and potentials was changed which confirmed low stability of the PTBs after 50 cycles. The results indicate that electropolymerization of PTBs has high stability during 10 scan rates. Therefore, this polymer is not a good matrix for successive applications after 50 cycles. So, PTBs, can be used in disposal usage.

3.7. Stability study of HRP(PSA) imprinted polymer

The stability of constructed bio-imprinted sensor was tested by DPV technique in 0.01 M of Fe $(CN)_6^{3-/4-}$ containing 0.1 M KCl. It is observed that the peak currents of the bio-imprinted sensor were decreased to 48.6% after 4 days which store after 4 days storage in 4 °C (Fig. 12).

3.8. Selectivity study

One of the most important features of biosensors is it's the Specific recognition of molecular targets. The selectivity of the MIP based bio-sensor was investigated in the presence of Carbohydrate antigen 15-3 (CA15-3) and CA 125 (cancer antigen 125) in PBS (pH = 6.5) as interfering substances. As shown in Fig. 13 the peak currents of the MIP/PTBs/GCE was tested by DPV technique in potential range of −0.8 to 1 V in Fe$(CN)_6^{3-/4-}$ containing KCl(0.1 M) solutions. According to the obtained results, the specific recognition of target HRP-PSA was highest than two other inference substances which indicate the obtained bio imprinted polymer has high selectivity. The reason of this results is a unique molecular structure of imprinted cavities which are proportional to the shape and size of target.

4. Conclusions

In summary, a facile, simple and cost-effective bio-imprinted polymer was constructed based of electropolymerization of toluidine blue and self-immobilization of enzyme-conjugated antigen on glass carbon electrode. The engineered imprinted biosensor exhibit catalytic activity toward hydrogen peroxide. Toluidine blue was used as the supporting substrate which enhances the large surface area for efficient rebinding of HRP(PSA). Under the optimized operating conditions, the proposed bio-imprinted polymer presents highly linear range for reduction of H_2O_2 from 0.001 to 40 mM with the low limit of quantitation (LLOQ) 0.001 mM. The successful fabrication of the biological imprinted polymer is due to an increase in active surface area, high electrical conductivity and fast electron transfer of obtained PTBs as matrix polymer which support efficient binding of HRP(PSA) on electrode. Obtained results indicate that the proposed methods can be used for fabricating other bio-macromolecules imprinted polymer and has application potential in clinical and biomedical analysis.

Acknowledgements

This research work was supported by Azarbaijan Shahid Madani University and Tabriz University of Medical Sciences.

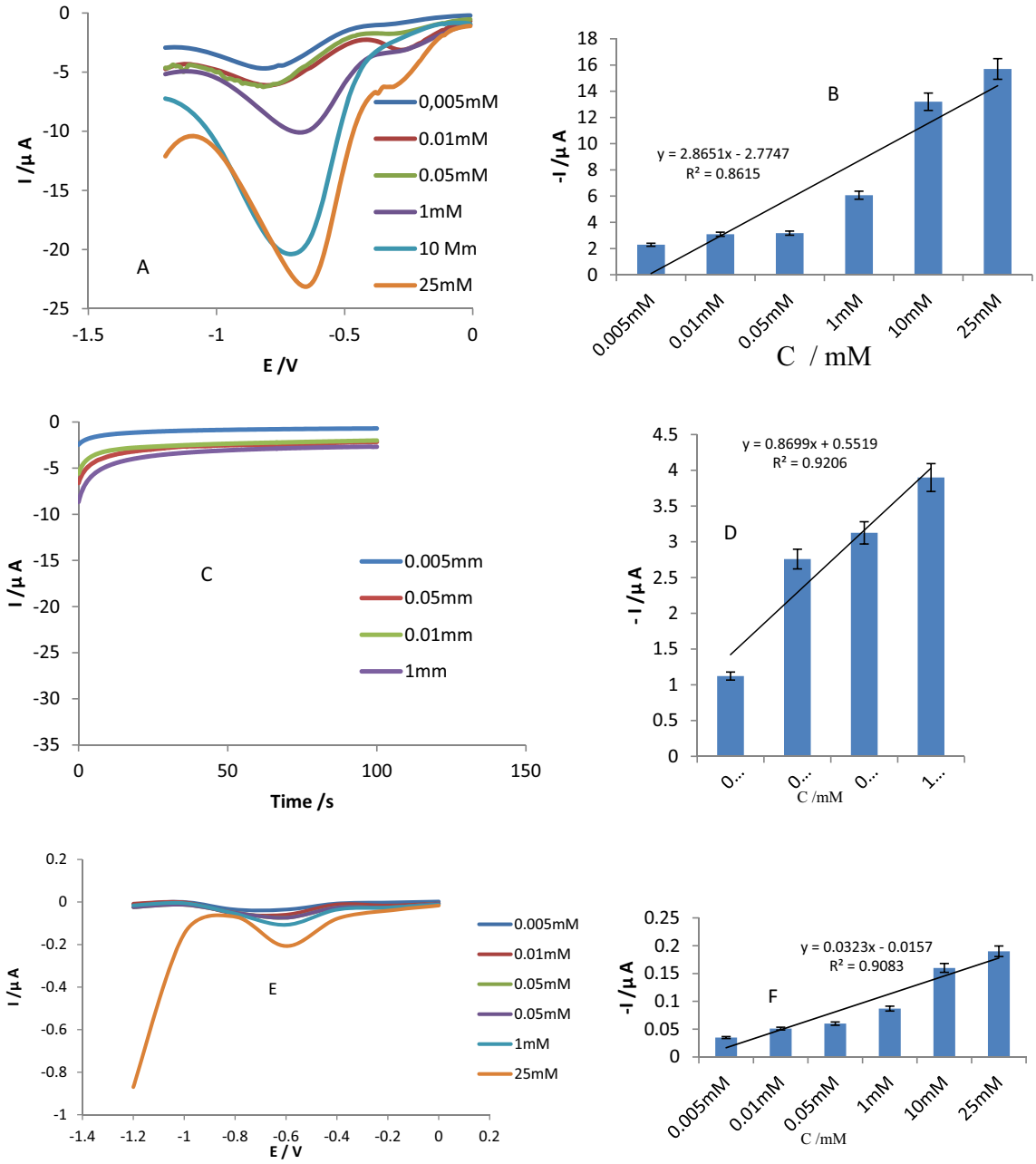

Fig. 10. A) SWVs, C) chronoamperometry, and E) DPVs of the HRP(PSA)/PTBs-based biosensor for detection of H_2O_2 in human plasma samples in different concentration. (B, D, and F) Calibration curves of SWVs, chronoamperometry, and DPVs, respectively.

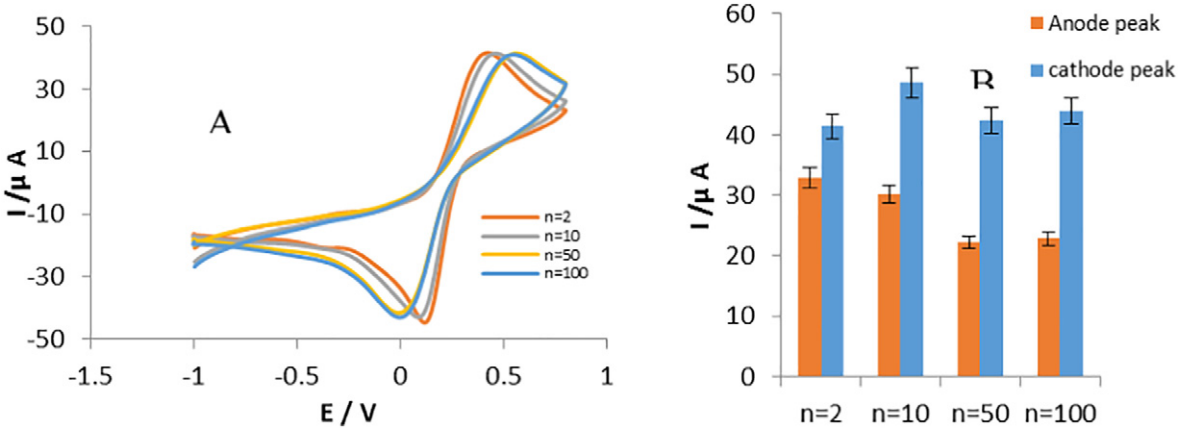

Fig. 11. A) CVs of PTBs/GCE in different cycle numbers (2, 10, 50, 100 cycles). B) Histogram of the redox peak currents *versus* number of cycles. Scan rate: 50 mV/s.

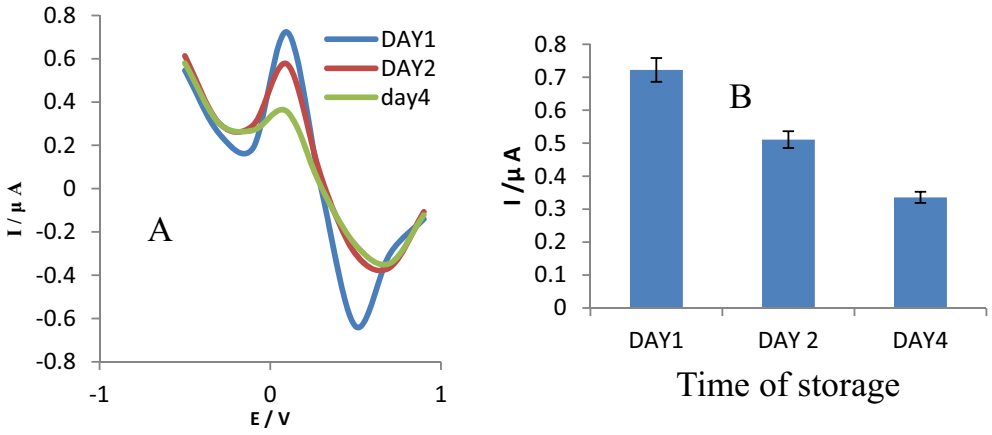

Fig. 12. A) DPVs and B) histograms for the stability study of HRP(PSA)/PTBs/GCE in the potential range of −0.8 to 1 and sweep 50 mV/s in 1 mM of Fe $(CN)_6^{3-/4-}$. In different storage times.

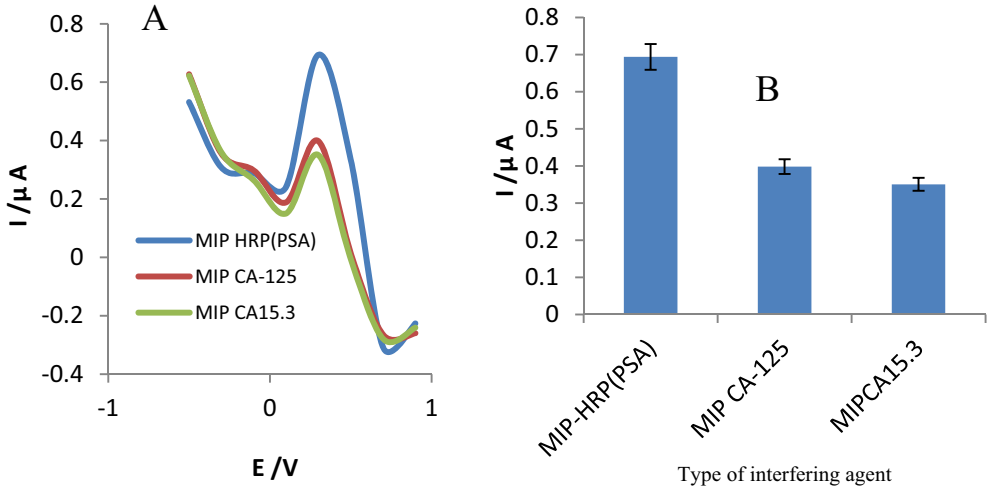

Fig. 13. (A) DPVs of MIP/PTBs/GCE in the presence of CA-15.3 and CA-125 as interfering agent. B) Histogram of peak currents *versus* type of interfering species.

References

[1] G. Ertürk, B. Mattiasson, From imprinting to microcontact imprinting-a new tool to increase selectivity in analytical devices, J. Chromatogr. B 1021 (2016) 30–44.
[2] P. Luliński, Molecularly imprinted polymers based drug delivery devices: a way to application in modern pharmacotherapy. A review, Mater. Sci. Eng. C 76 (2017) 1344–1353.
[3] J. Li, S. Li, Z. He, Molecular imprinting functionalized silica xerogel for selective recognition of levorotatory ofloxacin, Mater. Sci. Eng. C 71 (2017) 999–1003.
[4] A. Sorribes-Soriano, F. Esteve-Turrillas, S. Armenta, M. de la Guardia, J. Herrero-Martínez, Cocaine abuse determination by ion mobility spectrometry using molecular imprinting, J. Chromatogr. A 1481 (2017) 23–30.
[5] S. Li, M. Zhu, M.J. Whitcombe, S.A. Piletsky, A.P. Turner, Molecularly Imprinted Polymers for Enzyme-like Catalysis: Principle, Design, and Applications. Molecularly Imprinted Catalysts, Elsevier, 2016 1–17.
[6] Z. Cheng, L. Zhang, Y. Li, Synthesis of an enzyme-like imprinted polymer with the substrate as the template, and its catalytic properties under aqueous conditions, ChemistryA European Journal 10 (14) (2004) 3555–3561.
[7] X. Que, B. Liu, L. Fu, J. Zhuang, G. Chen, D. Tang, Molecular imprint for electrochemical detection of streptomycin residues using enzyme signal amplification, Electroanalysis 25 (2) (2013) 531–537.
[8] B. Liu, D. Tang, B. Zhang, X. Que, H. Yang, G. Chen, Au(III)-promoted magnetic molecularly imprinted polymer nanospheres for electrochemical determination of streptomycin residues in food, Biosens. Bioelectron. 41 (2013) 551–556.
[9] N. Leibl, Development of Molecularly Imprinted Polymers for Chemical Sensors, 2018.
[10] Y. Suga, H. Sunayama, T. Ooya, T. Takeuchi, Molecularly imprinted polymers prepared using protein-conjugated cleavable monomers followed by site-specific post-imprinting introduction of fluorescent reporter molecules, Chem. Commun. 49 (76) (2013) 8450–8452.
[11] A. Bossi, S.A. Piletsky, E.V. Piletska, P.G. Righetti, A.P. Turner, Surface-grafted molecularly imprinted polymers for protein recognition, Anal. Chem. 73 (21) (2001) 5281–5286.
[12] M.J. Whitcombe, I. Chianella, L. Larcombe, S.A. Piletsky, J. Noble, R. Porter, et al., The rational development of molecularly imprinted polymer-based sensors for protein detection, Chem. Soc. Rev. 40 (3) (2011) 1547–1571.
[13] M.F. Frasco, L.A. Truta, M.G.F. Sales, F.T. Moreira, Imprinting technology in electrochemical biomimetic sensors, Sensors 17 (3) (2017) 523.
[14] O. Ramström, K. Mosbach, Synthesis and catalysis by molecularly imprinted materials, Curr. Opin. Chem. Biol. 3 (6) (1999) 759–764.
[15] K. Flavin, M. Resmini, Imprinted nanomaterials: a new class of synthetic receptors, Anal. Bioanal. Chem. 393 (2) (2009) 437–444.
[16] N. Shah, M. Ul-Islam, M. Haneef, J.K. Park, A brief overview of molecularly imprinted polymers: from basics to applications, J. Pharm. Res. 5 (6) (2012) 3309–3317.
[17] H. Yan, K. Row, Characteristic and synthetic approach of molecularly imprinted polymer, Int. J. Mol. Sci. 7 (5) (2006) 155–178.
[18] G. Vasapollo, R.D. Sole, L. Mergola, M.R. Lazzoi, A. Scardino, S. Scorrano, et al., Molecularly imprinted polymers: present and future prospective, Int. J. Mol. Sci. 12 (9) (2011) 5908–5945.
[19] E. Verheyen, J.P. Schillemans, M. van Wijk, M.-A. Demeniex, W.E. Hennink, C.F. van Nostrum, Challenges for the effective molecular imprinting of proteins, Biomaterials 32 (11) (2011) 3008–3020.
[20] N.M. Maier, W. Lindner, Chiral recognition applications of molecularly imprinted polymers: a critical review, Anal. Bioanal. Chem. 389 (2) (2007) 377–397.
[21] H. Duan, X. Wang, Y. Wang, J. Li, Y. Sun, C. Luo, An efficient horseradish peroxidase chemiluminescence biosensor with surface imprinting based on phenylboronic acid functionalized ionic liquid@ magnetic graphene oxide, Sensors Actuators B Chem. 236 (2016) 44–51.
[22] Y. Liu, B. Cao, P. Jia, J. An, C. Luo, L. Ma, et al., Layer-by-layer surface molecular imprinting on polyacrylonitrile nanofiber mats, J. Phys. Chem. A 119 (25) (2015) 6661–6667.
[23] Y. Tian, Y. Wang, S. Wu, Z. Sun, B. Gong, Preparation of ampicillin surface molecularly imprinted polymers for its selective recognition of ampicillin in eggs samples, Int. J. Anal. Chem. 2018 (2018).
[24] Z. Wang, F. Li, J. Xia, L. Xia, F. Zhang, S. Bi, et al., An ionic liquid-modified graphene based molecular imprinting electrochemical sensor for sensitive detection of bovine hemoglobin, Biosens. Bioelectron. 61 (2014) 391–396.

[25] A. Barozet, M. Bianciotto, T. Siméon, H. Minoux, J. Cortés, Conformational changes in antibody Fab fragments upon binding and their consequences on the performance of docking algorithms, Immunol. Lett. 200 (2018) 5–15.
[26] Q. Wang, R. Xue, H. Guo, Y. Wei, W. Yang, A facile horseradish peroxidase electrochemical biosensor with surface molecular imprinting based on polyaniline nanotubes, J. Electroanal. Chem. 817 (2018) 184–194.
[27] I. Sekine, K. Kohara, T. Sugiyama, M. Yuasa, Syntheses of polymerized films on mild steels by electro-oxidation and electroreduction and their corrosion resistance, J. Electrochem. Soc. 139 (11) (1992) 3090–3097.
[28] T. Tatsuma, Y. Yokoyama, D.A. Buttry, N. Oyama, Electrochemical polymerization and depolymerization of 2,5-dimercapto-1,3,4-thiadiazole. QCM and spectroscopic analysis, J. Phys. Chem. B 101 (38) (1997) 7556–7562.
[29] H. Satake, T. Sakata, Electropolymerized poly(toluidine blue O) film electrode for potentiometric biosensing, Sensors and Materials 30 (2018) 2333.
[30] A.A. Karyakin, E.E. Karyakina, W. Schuhmann, H.L. Schmidt, S.D. Varfolomeyev, New amperometric dehydrogenase electrodes based on electrocatalytic NADH-oxidation at poly (methylene blue)-modified electrodes, Electroanalysis 6 (10) (1994) 821–829.
[31] S. Gandolfo, M. Pentenero, R. Broccoletti, M. Pagano, M. Carrozzo, C. Scully, Toluidine blue uptake in potentially malignant oral lesions in vivo: clinical and histological assessment, Oral Oncol. 42 (1) (2006) 88–94.
[32] L.M. Lu, S.P. Wang, F.L. Qu, X.B. Zhang, S. Huan, G.L. Shen, et al., Synthesis and characterization of poly (toluidine blue) nanowires and their application in amperometric biosensors, Electroanalysis 21 (10) (2009) 1152–1158.
[33] C.-X. Cai, K.-H. Xue, Electrochemical polymerization of toluidine blue o and its electrocatalytic activity toward NADH oxidation, Talanta 47 (5) (1998) 1107–1119.
[34] Y. Lv, T. Tan, F. Svec, Molecular imprinting of proteins in polymers attached to the surface of nanomaterials for selective recognition of biomacromolecules, Biotechnol. Adv. 31 (8) (2013) 1172–1186.
[35] Y.C. Chang, J.H. Jong, G.T.K. Fey, Kinetic characterization of the electrochemical intercalation of lithium ions into graphite electrodes, J. Electrochem. Soc. 147 (6) (2000) 2033–2038.
[36] M. Hasanzadeh, E. Solhi, M. Jafari, A. Mokhtarzadeh, J. Soleymani, A. Jouyban, et al., Ultrasensitive immunoassay of tumor protein CA 15.3 in MCF-7 breast cancer cell lysates and unprocessed human plasma using gold nanoparticles doped on the structure of mesoporous silica, Int. J. Biol. Macromol. 120 (2018) 2493–2508.
[37] A. Mirzaie, A. Saadati, A. Hassanpour, M. Hasanzadeh, M.R. Siahi-Shadbad, A. Jouyban, Determination of proline in human plasma samples using the encapsulation of proline dehydrogenase enzyme in dendritic silica: a new platform for the enzymatic biosensing of amino acids, Ana. Methods 11 (36) (2019) 4609–4619.
[38] W. Koros, D. Punsalan, Polymer Glasses: Diffusion in, 2001.
[39] J. Xu, F. Shang, J.H. Luong, K.M. Razeeb, J.D. Glennon, Direct electrochemistry of horseradish peroxidase immobilized on a monolayer modified nanowire array electrode, Biosens. Bioelectron. 25 (6) (2010) 1313–1318.
[40] J. Kaerger, D.M. Ruthven, Diffusion in nanoporous materials: fundamental principles, insights and challenges, New J. Chem. 40 (5) (2016) 4027–4048.
[41] T.L. Poulos, Heme enzyme structure and function, Chem. Rev. 114 (7) (2014) 3919–3962.
[42] P. Rich, M. Iwaki, A comparison of catalytic site intermediates of cytochrome c oxidase and peroxidases, Biochem. Mosc. 72 (10) (2007) 1047.